

Final Report (AOARD-06-4013)

**Nonlinear Response Structural Optimization
of a Joined-Wing Using Equivalent Loads**

Gyung-Jin Park

Professor
Department of Mechanical Engineering
Hanyang University
1271 Sa-1 Dong, Sangnok-gu, Ansan City,
Gyeonggi-do 426-791, Korea

April 2007

Report Documentation Page

Form Approved
OMB No. 0704-0188

Public reporting burden for the collection of information is estimated to average 1 hour per response, including the time for reviewing instructions, searching existing data sources, gathering and maintaining the data needed, and completing and reviewing the collection of information. Send comments regarding this burden estimate or any other aspect of this collection of information, including suggestions for reducing this burden, to Washington Headquarters Services, Directorate for Information Operations and Reports, 1215 Jefferson Davis Highway, Suite 1204, Arlington VA 22202-4302. Respondents should be aware that notwithstanding any other provision of law, no person shall be subject to a penalty for failing to comply with a collection of information if it does not display a currently valid OMB control number.

1. REPORT DATE 15 NOV 2007		2. REPORT TYPE		3. DATES COVERED	
4. TITLE AND SUBTITLE Nonlinear Response Optimization Using Equivalent Loads for a Joined-Wing				5a. CONTRACT NUMBER	
				5b. GRANT NUMBER	
				5c. PROGRAM ELEMENT NUMBER	
6. AUTHOR(S) Gyung-Jin Park				5d. PROJECT NUMBER	
				5e. TASK NUMBER	
				5f. WORK UNIT NUMBER	
7. PERFORMING ORGANIZATION NAME(S) AND ADDRESS(ES) Hanyang University, 1271 Sa 1-Dong, Ansan, Gyunggi-Do, Korea (South), KS, 426-791				8. PERFORMING ORGANIZATION REPORT NUMBER N/A	
9. SPONSORING/MONITORING AGENCY NAME(S) AND ADDRESS(ES)				10. SPONSOR/MONITOR'S ACRONYM(S)	
				11. SPONSOR/MONITOR'S REPORT NUMBER(S)	
12. DISTRIBUTION/AVAILABILITY STATEMENT Approved for public release; distribution unlimited.					
13. SUPPLEMENTARY NOTES					
14. ABSTRACT Final report of research in geometric nonlinear response optimization of a joined-wing, carried out by using equivalent loads. The utilized structure is a joined-wing that is currently being developed in the US Air Force Research Laboratories (AFRL). The joined-wing is modeled for finite element analysis (FEA). Equivalent loads are the load sets which generate the same response field in linear analysis as that from nonlinear analysis.					
15. SUBJECT TERMS					
16. SECURITY CLASSIFICATION OF:			17. LIMITATION OF ABSTRACT	18. NUMBER OF PAGES 37	19a. NAME OF RESPONSIBLE PERSON
a. REPORT unclassified	b. ABSTRACT unclassified	c. THIS PAGE unclassified			

Abstract

The joined-wing is a new concept of the airplane wing. The fore-wing and the aft-wing are joined together in the joined-wing. The range and loiter are longer than those of a conventional wing. The joined-wing can lead to increased aerodynamic performances and reduction of the structural weight. The structural behavior of the joined-wing has a high geometric nonlinearity according to the external loads. The gust loads are the most critical loading conditions in the structural design of the joined-wing. The nonlinear behavior should be considered in the optimization of the joined-wing. It is well known that conventional nonlinear response optimization is extremely expensive; therefore, the conventional method is almost impossible to use in large scale structures such as the joined-wing.

In this research, geometric nonlinear response optimization of a joined-wing is carried out by using equivalent loads. The utilized structure is a joined-wing that is currently being developed in the US Air Force Research Laboratories (AFRL). The joined-wing is modeled for finite element analysis (FEA). Equivalent loads are the load sets which generate the same response field in linear analysis as that from nonlinear analysis. In the equivalent loads method, the external loads are transformed to the equivalent loads (EL) for linear static analysis, and linear response optimization is carried out based on the EL. The design is updated by

the results of linear response optimization. Nonlinear analysis is carried out again and the process proceeds in a cyclic manner until the convergence criteria are satisfied. In other words, nonlinear response optimization is conducted by repeated use of linear response optimization. It has been verified that the equivalent loads method is equivalent to a gradient-based method; therefore, the solution is the same as that of exact nonlinear response optimization.

Table of Contents

Abstract	2
Table of Contents	i
LIST OF FIGURES	ii
LIST OF TABLES	iii
1 Introduction	1
2 Nonlinear structural optimization using equivalent loads.....	4
2.1 Calculation of equivalent loads.....	4
2.2 The steps for nonlinear response structural optimization using equivalent loads (NROEL).....	7
3 Analysis of the joined-wing	8
3.1 Finite element modeling of the joined-wing	8
3.2 Loading conditions of the joined-wing	9
3.3 Boundary conditions of the joined-wing.....	10
3.4 Geometric nonlinearity of the joined-wing	10
4 Structural optimization of the joined-wing	12
4.1 Definition of design variables	12
4.2 Formulation.....	12
4.3 Programming for the equivalent loads method	13
5 Discussion	14
5.1 Results of linear response optimization	14
5.2 Results of nonlinear response optimization	14
5.3 Discussion	15
6 Conclusions.....	17
References.....	29

LIST OF FIGURES

- Fig. 1 Configuration of the joined-wing
- Fig. 2 Generation of equivalent loads for displacement constraints
- Fig. 3 Generation of equivalent loads for stress constraints
- Fig. 4 Optimization process using the equivalent static loads
- Fig. 5 Finite element modeling of the joined-wing
- Fig. 6 Boundary conditions of the joined-wing
- Fig. 7 Deformation of the joined-wing under the gust loading condition
- Fig. 8 Stress contours from linear analysis of a joined-wing
- Fig. 9 Stress contours from nonlinear analysis of a joined-wing
- Fig. 10 History of linear response optimization
- Fig. 11 History of nonlinear response optimization
- Fig. 12 Thickness contour of linear response optimization result
- Fig. 13 Stress contours from linear analysis of the linear optimization result
- Fig. 14 Thickness contour of nonlinear response optimization result
- Fig. 15 Deformation of the optimum design
- Fig. 16 Stress contours from nonlinear analysis of the optimum design
- Fig. 17 Critical buckling mode for the cruise speed gust loading condition

LIST OF TABLES

- Table 1 Loading conditions for optimization
- Table 2 Wing tip displacements of the linear and nonlinear analyses
- Table 3 Results of linear response optimization
- Table 4 Results of nonlinear response optimization

1 Introduction

The joined-wing airplane may be defined as an airplane that incorporates tandem wings arranged to form diamond shapes in both plan and front views. Figure 1 shows a general joined-wing aircraft. The fore-wing and aft-wing are joined in the joined-wing. Wolkobitch published the joined-wing concept in 1986. ⁽¹⁾ The joined-wing has the advantage of a longer range and loiter than that of a conventional wing. Generally, the weight of the joined-wing aircraft is lighter than that of a conventional wing. Miura, Shyu and Wolkobitch used an optimization method to study the effects of joined-wing geometry parameters on structural weight. ⁽²⁾ Gallman and Kroo offered many recommendations for the design methodology of a joined-wing. ⁽³⁾ They used the fully stressed design (FSD) for optimization. Blair and Canfield initiated nonlinear exploration on a joined-wing configuration in 2005. ⁽⁴⁾ Air Force Research Laboratories (AFRL) have been developing an airplane with the joined-wing to complete a long-endurance surveillance mission. ⁽⁴⁻⁸⁾ Lee et al. performed dynamic response structural optimization of a joined-wing using equivalent static loads. They considered the dynamic effect of the joined-wing in the optimization. ⁽⁹⁾

The joined-wing has a high geometric nonlinearity. ⁽⁴⁾ Geometric nonlinearity should be considered when deformation is large enough so that the equilibrium equations must be written with respect to the deformed structural geometry. Also, the loads may change the directions as they increase. ⁽¹¹⁾ Generally, the applied loads act vertically as a lifting force

for the joined-wing. The displacement of the wing-tip becomes very large as the applied loads increase. The load directions are changed due to the large deformation of the joined-wing. Therefore, the followed force, which is the force at the last stage of the deformation, should be considered.

Gust is the movement of the air in turbulence and the gust load has a large impact on the airplane.⁽¹⁴⁾ The gust loads are the most important loading conditions when an airplane wing is designed. The gust loads for a joined-wing have been calculated by the researchers of the Air Force Research Laboratory.⁽⁴⁾ Static loads for the gust can be generated from an aeroelastic model which uses the Panel method.⁽¹⁰⁾

During the past decades, many finite element theories considering nonlinearity have been developed and applied to practical problems.⁽¹¹⁻¹³⁾ However, it is not easy to mathematically optimize a structure with nonlinear behavior because calculation of nonlinear sensitivity is extremely difficult or expensive.⁽¹⁵⁻¹⁷⁾ Sensitivity information is used to make the decision of the direction of the design change.⁽¹⁸⁻²⁰⁾ In a nonlinear system, a linear relationship between the external force and structural behavior cannot be expected. Therefore, many nonlinear analyses are required in the optimization process.

In previous research, Blair et al. performed nonlinear structural optimization of a joined-wing using a fully stressed design (FSD).⁽⁴⁾ FSD is a non-gradient based algorithm that is used for resizing element thicknesses or areas so as to produce a design where each designed property is subjected to its maximum allowable stress. FSD provides a rapid means of performing initial sizing of aerospace vehicles and allows for the

design of a virtually unlimited number of element sizes. However, the FSD method may not do as well when several materials are employed. Only thickness or area can be used as design variables. The FSD method is efficient for designing structures subject only to stress constraints. The solution of FSD is not as exact as that of the gradient based optimization method relatively.^(18, 21)

A modified gradient based optimization algorithm has been proposed for nonlinear response structural optimization. This algorithm is called nonlinear response optimization using equivalent loads (NROEL).⁽²¹⁻²³⁾ A nonlinear response optimization problem is converted to linear response optimization with equivalent loads. The original loads are changed to a set of equivalent loads based on the responses. The set of loads are used as multiple loading conditions of linear response optimization. The design is changed in linear response optimization. A new set of equivalent loads is made again and the process proceeds in a cyclic fashion until the convergence criteria are satisfied.

A finite element model for a joined-wing is established. Nonlinear finite element analysis is performed by considering geometric nonlinearity. As mentioned earlier, gust loads are critical in the joined-wing; therefore, the followed forces of the gusts are considered in the analysis. Structural optimization is performed to incorporate the results of nonlinear analysis. The NROEL method is employed for nonlinear response structural optimization. Size optimization for the thickness of each finite element is conducted to reduce the structural mass while design conditions are satisfied. ABAQUS is used for

nonlinear analysis and GENESIS is used for the linear response optimization process in NROEL.^(25,26)

2 Nonlinear structural optimization using equivalent loads

There are several methods for nonlinear structural optimization. The conventional gradient based method gives an excellent solution.⁽¹⁸⁻²⁰⁾ However, because the method is extremely expensive due to sensitivity analysis, it is not applicable to large scale problems. The FSD method and the response surface method (RSM) are non gradient based optimization algorithms.^(16,17) The solution of these methods is not as exact as that of the gradient based optimization method. Moreover, the RSM method cannot solve a large scale problem that has several hundreds of design variables. The NROEL method is a gradient based optimization algorithm and the joined-wing structure is optimized by NROEL in this research. The method is explained as follows:

2.1 Calculation of equivalent loads

The equivalent loads (EL) are defined as the loads for linear analysis, which generate the same response fields as those of nonlinear analysis. According to the finite element method⁽¹⁰⁻¹²⁾, the equilibrium equation of a structure with nonlinearity is

$$\mathbf{K}(\mathbf{b}, \mathbf{z}_N) \mathbf{z}_N = \mathbf{f} \quad (2-1)$$

where \mathbf{K} is the stiffness matrix which is the function of the design variable vector \mathbf{b} and the nodal displacement vector \mathbf{z} . The subscript N means that the displacement is obtained by nonlinear analysis. \mathbf{f} is the external load vector, \mathbf{z}_N is obtained from Eq. (2-1). The equivalent load for displacements is defined as:

$$\mathbf{f}_{eq}^z = \mathbf{K}_L(\mathbf{b}) \mathbf{z}_N \quad (2-2)$$

where \mathbf{f}_{eq}^z is the equivalent load vector for displacement, \mathbf{K}_L is the linear stiffness matrix and \mathbf{z}_N is the nodal displacement vector from Eq. (2-1). \mathbf{f}_{eq}^z is used in Eq. (2-3)

which is the equation of linear analysis using the finite element method as follows:

$$\mathbf{K}_L(\mathbf{b}) \mathbf{z}_L = \mathbf{f}_{eq}^z \quad (2-3)$$

where the nodal displacement vector \mathbf{z}_L has the same values as the nonlinear nodal displacement vector \mathbf{z}_N in Eq. (2-1). Therefore, if the equivalent load \mathbf{f}_{eq}^z is used as an external load in linear response optimization, the same displacements as the nonlinear response can be considered throughout linear response optimization. Figure 2 shows this process.

Although the load \mathbf{f}_{eq}^z can generate the same displacements as the nonlinear displacements, it does not generate the same stress responses. The equivalent load for the stresses can be separately calculated. The stress response $\boldsymbol{\sigma}_N$ is obtained from Eq. (2-1)

of nonlinear analysis. The obtained stress is used as the initial stress. Therefore, the equivalent load for stresses is calculated as follows:

$$\mathbf{K}_L(\mathbf{b})\mathbf{z}_L^\sigma = -\bar{\mathbf{f}}_I(\boldsymbol{\sigma}) \quad (2-4)$$

$$\mathbf{f}_{eq}^\sigma = \mathbf{K}_L(\mathbf{b})\mathbf{z}_L^\sigma \quad (2-5)$$

where \mathbf{f}_{eq}^σ is the equivalent load vector for the stress response, \mathbf{K}_L is the linear stiffness matrix of, $\boldsymbol{\sigma}_N$ from Eq. (2-1) is utilized as the initial stress effect $-\bar{\mathbf{f}}_I(\boldsymbol{\sigma})$ in Eq. (2-4) of linear analysis. \mathbf{z}_L^σ is the displacement vector from Eq. (2-4). \mathbf{f}_{eq}^σ can be calculated by multiplying \mathbf{K}_L and \mathbf{z}_L^σ as shown in Eq. (2-5). \mathbf{f}_{eq}^σ can be used as follows:

$$\mathbf{K}_L(\mathbf{b})\mathbf{z}_L = \mathbf{f}_{eq}^z \quad (2-6)$$

The stress response $\boldsymbol{\sigma}_L$ is obtained from Eq. (2-6) of linear analysis. This stress response may not exactly be the same as that from nonlinear analysis. The difference can be adjusted by $\hat{\boldsymbol{\sigma}}_L$ as shown in Figure 3. The stress vector $\hat{\boldsymbol{\sigma}}_L$ has the same stress as the nonlinear stress response. Therefore, if the equivalent load \mathbf{f}_{eq}^σ is used as an external load in linear optimization, the same stress with nonlinear stress can be considered throughout the linear response optimization process.

If the problem has a displacement constraint as well as a stress constraint, equivalent loads should be calculated with respect to each response, and the sets of the equivalent loads are utilized in linear response optimization as multiple loading conditions.

2.2 The steps for nonlinear response structural optimization using equivalent loads (NROEL)

The overall process of the NROEL algorithm is illustrated in Fig. 4. The steps of the algorithm are as follows:

Step 1. Set initial values and parameters (design variables: $\mathbf{b}^{(k)} = \mathbf{b}^{(0)}$, cycle number: $k = 0$, convergence parameter: a small number ε).

Step 2. Perform nonlinear analysis with $\mathbf{b}^{(k)}$. Hence the linear stiffness matrix and nonlinear responses are obtained.

Step 3. Calculate the equivalent load sets as follows:

$$\mathbf{f}_{eq}^{z,(k)} = \mathbf{K}_L(\mathbf{b})\mathbf{z}_N \quad \text{and} \quad \mathbf{f}_{eq}^{\sigma,(k)} = \mathbf{K}_L(\mathbf{b})\mathbf{z}_L^{\sigma} \quad (2-7)$$

Step 4. When $k = 0$, go to Step 5. When $k > 0$, if

$$\left\| \mathbf{f}_{eq}^{z,(k)} - \mathbf{f}_{eq}^{z,(k-1)} \right\| \leq \varepsilon \quad \text{and} \quad \left\| \mathbf{f}_{eq}^{\sigma,(k)} - \mathbf{f}_{eq}^{\sigma,(k-1)} \right\| \leq \varepsilon \quad (2-8)$$

then terminate the process. Otherwise, go to Step 5.

Step 5. Solve the following linear static response optimization problem:

$$\text{Find} \quad \mathbf{b}^{(k+1)} \quad (2-9a)$$

$$\text{to minimize} \quad f(\mathbf{b}^{(k+1)}) \quad (2-9b)$$

$$\text{subject to} \quad \mathbf{K}_L(\mathbf{b}^{(k+1)})\mathbf{z} - \mathbf{f}_{eq}^{z,(k)} = 0 \quad (2-9c)$$

$$\mathbf{K}_L(\mathbf{b}^{(k+1)})\mathbf{z} - \mathbf{f}_{eq}^{\sigma,(k)} = 0 \quad (2-9d)$$

$$g_j(\mathbf{b}^{(k+1)}, \mathbf{z}, \bar{\mathbf{c}}) \leq 0, \quad j = 1, \dots, m \quad (2-9e)$$

$$\mathbf{b}_{iL}^{(k+1)} \leq \mathbf{b}_i^{(k+1)} \leq \mathbf{b}_{iU}^{(k+1)}, \quad i = 1, \dots, n \quad (2-9f)$$

The external load \mathbf{f}_{eq} is the equivalent load vector. The two equivalent load sets are used as multiple loading conditions during the optimization process.

Step 6. Update the design results, set $k = k + 1$ and go to Step 2.

3 Analysis of the joined-wing

3.1 Finite element modeling of the joined-wing

The joined-wing consists of five parts, which are the fore-wing, the aft-wing, the mid-wing, the tip-wing and the edge around the joined-wing. The parts are illustrated in Figure 5. Each part is composed of the top skin, the bottom skin, the spar and the rib. The length from the wing-tip to the wing-root is 38 m and the length of the chord is 2.5 m. The model has 3027 elements with 2857 quadratic elements, 156 triangular elements and 14 rigid elements. Rigid elements make connections between the nodes of the aft-wing root with the center node of the aft-wing root. The structure has two kinds of aluminum materials. One has the Young's modulus of 72.4 GPa, the shear modulus of 27.6 GPa and the density 2770 kg/m³. The other has 36.2 GPa, 13.8 GPa and 2770 kg/m³, respectively. The latter material is used only for elements of the edge part. The former material is used for the entire elements except for the edge part. ⁽⁴⁾

3.2 Loading conditions of the joined-wing

Eleven loading conditions for structural optimization have been defined by the AFRL.

⁽⁴⁾ These loading conditions are composed of seven maneuver loads, two gust loads, one take-off load and one landing load as shown in Table 1. Each loading condition has a different loading direction and magnitude. The gust loading conditions are especially important in these loading conditions. Gust is the movement of the air in turbulence and the gust load has a large impact on the airplane. Static loads for the gust can be generated from an aeroelastic model which uses the Panel method. ⁽¹⁰⁾ The Panel method is used to calculate the velocity distribution along the surface of the airfoil. Panel methods have been developed to analyze the flow field around arbitrary bodies in two and three dimensions. The surface of the airfoil is divided into trapezoid panels. Mathematically, each panel induces a velocity on itself. This velocity can be expressed by relatively simple equations which contain geometric relations such as distances and angles between the panels only. The Panel method is referred as a boundary element method in some publications. ⁽¹⁰⁾ When the deformation is large the direction of an external force is changed according to the deformation. The followed force means the changed force for the deformation. As mentioned earlier, the followed forces at the last state of the deformation are utilized. ⁽⁴⁾

Linear and nonlinear response optimizations are performed in this research. All loading conditions are used for linear response optimization while only two gust loading conditions are used for nonlinear response optimization because the geometric nonlinearity

effect of the joined-wing largely occurs in the gust loading conditions. Relatively, a small nonlinear effect occurs in other loading conditions.

3.3 Boundary conditions of the joined-wing

The roots of the fore-wing and the aft-wing are joined to the fuselage. The entire part of the fore-wing root is attached to the fuselage. Therefore, all the degrees of freedom in six directions are fixed. On the other hand, the aft-wing root can be rotated with respect to the y -axis in Fig. 6. The boundary nodes of the aft-wing root are rigidly connected to the center node. The center node has an enforced rotation with respect to the y -axis. The boundary nodes are set free in the x and z translational directions. Other degrees of freedom are fixed. The enforced rotation generates torsion on the aft-wing and has quite an important aerodynamic effect. The amounts of the enforced rotation are from -0.0897 radian to 0 radian.⁽⁴⁾ These rotational values are different in each mission leg. The boundary conditions are illustrated in Fig. 6.

3.4 Geometric nonlinearity of the joined-wing

Linear and nonlinear analyses are performed under all loading conditions. The design data are adopted from a reference⁽⁴⁾ and the data are used for the initial design of the later optimization process. Table 2 shows the results of the analyses. As shown in Table 2, the wing tip displacement from nonlinear analysis is larger than that of linear analysis. In particular, the difference of the wing tip displacements between linear and nonlinear

analyses is quite large under the gust loading conditions.

We can see the highly geometric nonlinearity of the joined-wing. Therefore, nonlinear analysis and nonlinear response optimization are required for the joined-wing design. Figure 7 illustrates the deformed shape of the joined-wing under the maneuver speed gust loading condition. The wing tip displacement of nonlinear analysis is about five times larger than that of linear analysis. Figures 8 and 9 illustrate the stress contours of the joined-wing under the maneuver speed gust loading condition. On the whole, large stress occurs at the root of the aft-wing. The stresses from nonlinear analysis are quite larger than those from linear analysis. The maximum stress is about 3.56 GPa in the nonlinear analysis under the maneuver speed gust loading condition. This value is very large in the view of the fact that the maximum stress of linear analysis under the maneuver speed gust loading condition is 231 MPa. Moreover, it is larger than the allowable stress 179 MPa.

Buckling analysis is performed under all loading conditions. The critical buckling rates for the maneuver gust and cruise speed gust conditions are 74% and 67% of the gust load, respectively. The buckling primarily occurs at the aft wing. The critical buckling rate of the taxi crater impact load is 108%. The buckling rates of other maneuver loads are 166% and higher. When the buckling rate is more than 100%, the buckling safety is satisfied. Therefore, the buckling safety is not satisfied by the initial design.

4 Structural optimization of the joined-wing

4.1 Definition of design variables

As mentioned earlier, the FEM model has 3027 elements. Each element thickness is a design variable. But the edge part and rigid beams of the aft-wing root are not used as design variables. Therefore, the number of design variables is 2559. The upper and lower bounds are defined for each part. 0.001016 m, 0.0001277 m and 0.000254 m are used as the lower bounds of the skin part, the tip wing spar part, and other wing spars and the rib part, respectively. 0.3 m is used as the upper bounds of all the parts.

4.2 Formulation

The optimization problem is formulated as

$$\text{Find } t_i \quad (i = 1, \dots, 2559) \quad (4-1a)$$

$$\text{to minimize } \text{Mass} \quad (4-1b)$$

$$\text{subject to } |\sigma_j| \leq \sigma_{allowable} \quad (j = 1, \dots, 2559) \quad (4-1c)$$

$$0.001016 \text{ m} \leq t_{skin \ part} \leq 0.3 \text{ m} \quad (4-1d)$$

$$0.000127 \text{ m} \leq t_{tip \ wing \ part} \leq 0.3 \text{ m} \quad (4-1e)$$

$$0.000254 \text{ m} \leq t_{wing \ spars \ and \ ribs} \leq 0.3 \text{ m} \quad (4-1f)$$

The mass of the initial model is 3832 kg. First, linear response optimization is carried out for the initial model. Second, the optimum of the linear response optimization is the

initial design of nonlinear response optimization. The material of the joined-wing is aluminum. The allowable von Mises stress for aluminum is set by 269MPa. Since the safety factor 1.5 is used, the allowable stress is reduced to 179MPa.⁽⁴⁾ Stresses of all the elements except for the edge part should be less than the allowable stress, 179MPa.

4.3 Programming for the equivalent loads method

In this research, ABAQUS⁽²⁵⁾ is used for nonlinear response analysis and GENESIS⁽²⁶⁾ is used for linear response optimization. The two systems should be interfaced for nonlinear response optimization. The interface procedure is programmed by the C language.⁽²⁷⁾ To evaluate the equivalent loads in Eq. (2), we need the linear stiffness matrix and the nonlinear response. They are generated by ABAQUS and obtained by reading the output files of ABAQUS. The calculated equivalent loads are used as input to GENESIS; therefore, the loads are written on the input file for GENESIS. Moreover, the iterative process is controlled based on the convergence criteria. These capabilities are coded and the entire process automatically proceeds.

5 Discussion

5.1 Results of linear response optimization

Linear response optimization is performed under all loading conditions. The results from linear response optimization are shown in Table 3 and Fig. 10. The maximum stress of the initial model is 220.8% of the allowable stress; therefore, the stress constraints are violated. As expected, the maximum stress and displacement occurs at the gust loading condition. After the linear optimization, all the stress constraints are satisfied. Mass is increased by 16.8%. In linear analysis, the maximum displacement of the initial model is 4.62 m at the wing-tip while that of the optimum model is 4.25 m. The total number of iterations is six. GENESIS 7.0 is used for linear response structural optimization of the joined-wing.⁽²⁶⁾ As mentioned earlier, the total number of design variables is 2559 and the stresses of all elements except for the edge part are used as constraints. The Total CPU time for the linear response structural optimization is 45 hours using HP-UX Itanium II.⁽²⁸⁾

5.2 Results of nonlinear response optimization

Nonlinear response optimization is performed using equivalent loads for the gust loading conditions. The equivalent loads are generated for loading conditions 8 and 9 (gust) in Table 1. The optimum design of linear response optimization is used as the

initial design. The results from nonlinear response optimization are shown in Table 4 and Fig. 11.

When nonlinear analysis considering geometric nonlinearity is performed by the optimum of linear response optimization, the stress constraints are violated up to 1551.6%. Thus, linear optimization is not sufficient for the design of the joined-wing with highly geometric nonlinearity. After nonlinear response optimization, all the stress constraints are satisfied. The maximum stress of the optimum design is 178.97 MPa and the wing tip displacement is 3.458 m. Mass is increased by 58.3%. The total number of cycles is thirty one. This means that only thirty one nonlinear analyses are performed for the nonlinear response optimization with several thousand design variables. Abaqus 6.4 and GENESIS 7.0 are used for nonlinear analysis and linear response structural optimization of the joined-wing, respectively.^(25,26) The Total CPU time for nonlinear response structural optimization is 335 hours using HP-UX Itanium II.⁽²⁸⁾

5.3 Discussion

When nonlinear analysis is performed, the optimum design from linear response optimization violates the stress constraints. It has been shown through linear and nonlinear analyses that highly geometric nonlinearity is involved in the joined-wing. The difference of the wing-tip displacement is quite large between linear analysis and nonlinear analysis. The difference of the maximum value and distribution of stress is also fairly large.

After linear response optimization, the contour of optimum thickness is illustrated in Fig. 12. The thickness of the aft-wing is large in the leading edge part of the top skin and the trailing edge part of the bottom skin. The stress contour of the optimum design is illustrated in Fig. 13. The critical stress occurs at the aft-wing part as well as the mid-wing part.

The contour of the optimum thickness of nonlinear response optimization is illustrated in Fig. 14. The thickness of the aft-wing is quite large in the leading edge part of the top skin and the trailing edge part of the bottom skin. This result is similar to that of linear response optimization. However, the thicknesses are larger than those of linear response optimization.

On the whole, the thickness of nonlinear response optimization is larger than that of linear response optimization. In the two optimizations, the maximum stress occurs at the aft-wing. Tip wing elements are thin, and the aft-wing spar has the maximum thickness. In linear response optimization, the middle position of the aft-wing spar has the maximum thickness. On the other hand, the wing root position of the aft-wing spar has the maximum thickness in nonlinear response optimization. The analysis results of linear and nonlinear analysis are fairly different because the direction and the magnitude of the loads are changed according to the deformation of the structure in geometric nonlinear analysis. The optimization results are different accordingly. Therefore, nonlinear response structural optimization is needed when a structure has a high nonlinearity. Figures 15 and

16 illustrate the deformation and stress contour of the optimum design of nonlinear response optimization, respectively.

Buckling analysis is performed for the optimized design. The negative buckling mode occurs in several loading conditions. This means that buckling occurs when the load is reversed. Negative buckling mode was neglected in this discussion. The most critical buckling rate for the taxi crater impact loading conditions is 171%. The critical buckling rates for the maneuver and cruise speed gust loading conditions are 210% and 187%, respectively. The buckling rate of other loading conditions is 445% or higher. The critical buckling mode for the cruise speed gust loading condition is shown in Fig. 17. It is noted that the optimization process does not consider the buckling constraint. However, the buckling constraint is satisfied by the optimized design. In the future, we need to include the buckling constraint.

6 Conclusions

A joined-wing which has a longer range and loiter than a conventional wing is investigated from the viewpoint of weight reduction. The joined-wing configuration exhibits large geometric nonlinearity under the critical gust load conditions. Moreover, the gust load is the most important in design. Thus, nonlinear analysis under the gust loading condition is required for the design of the joined-wing.

The joined-wing structure is optimized. The structure has many design variables. When a design problem is large, nonlinear response structural optimization is very difficult because a large amount of efforts is required to calculate the sensitivity information. The equivalent loads method is used as a gradient based optimization method. The equivalent loads method is a very efficient method in that the nonlinear response sensitivity is not required. Equivalent loads are defined as the loads for linear analysis, which generate the same response field as that of nonlinear analysis. A gradient based optimization method for linear response optimization is used in an iterative manner. Moreover, the equivalent loads method can be applied to large scale problems such as a problem with several thousand design variables and constraints.

The optimum design considering geometric nonlinearity of the joined-wing satisfies all the stress constraints. Although the optimization process does not consider the buckling constraint, the buckling property is improved. The results from nonlinear response optimization and linear response optimization are compared. It is presented that the optimum design from linear response optimization may not be safe for a highly nonlinear problem. In future work, nonlinear transient response optimization of the joined-wing will be performed using equivalent static loads. The nonlinear effect as well as the dynamic effect will be considered.

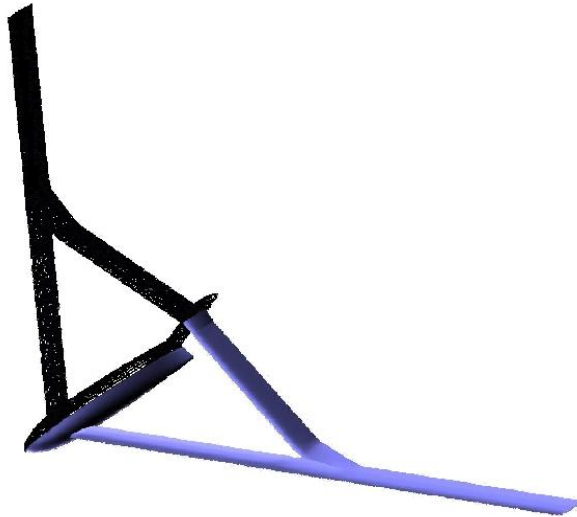


Fig. 1 Configuration of the joined-wing

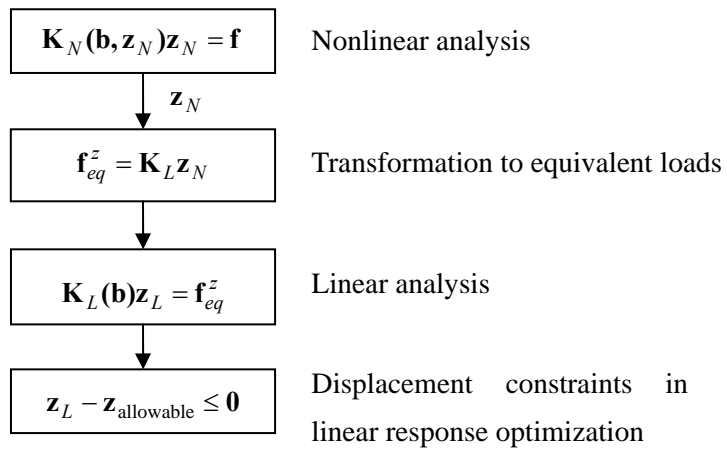


Fig. 2 Generation of equivalent loads for displacement constraints

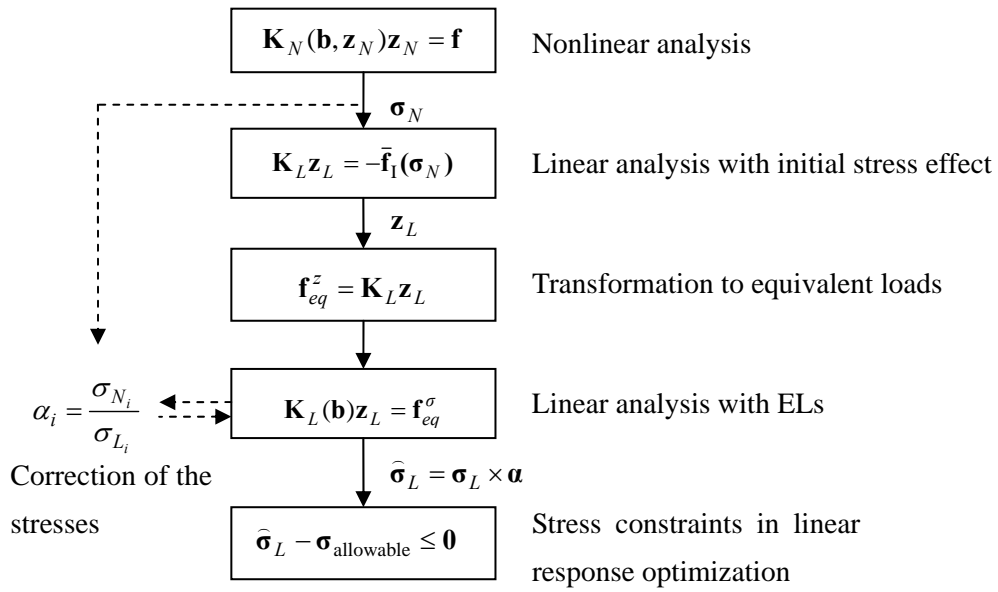


Fig. 3 Generation of equivalent loads for stress constraints

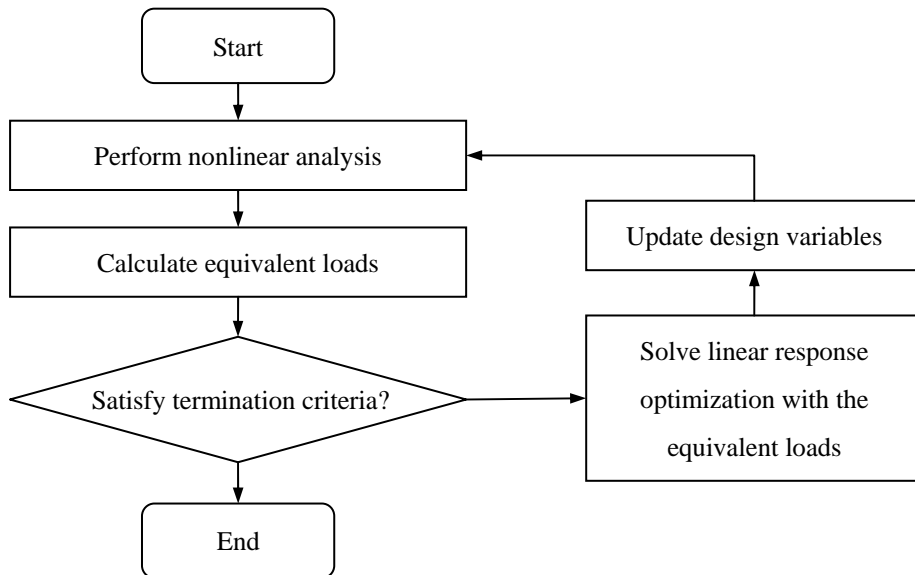


Fig. 4 Optimization process using the equivalent static loads

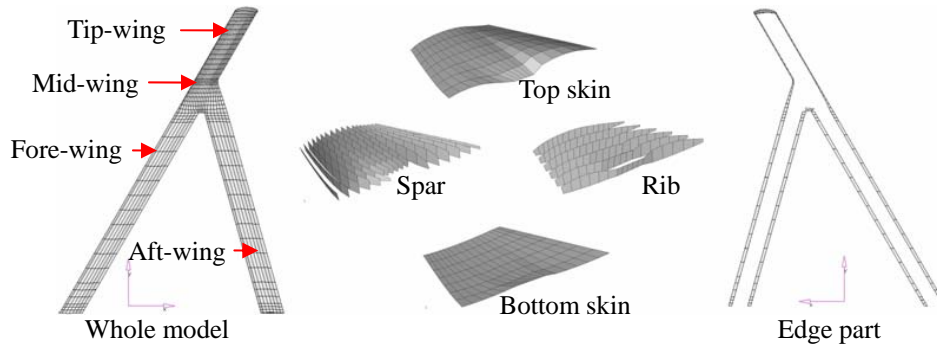


Fig. 5 Finite element modeling of the joined-wing

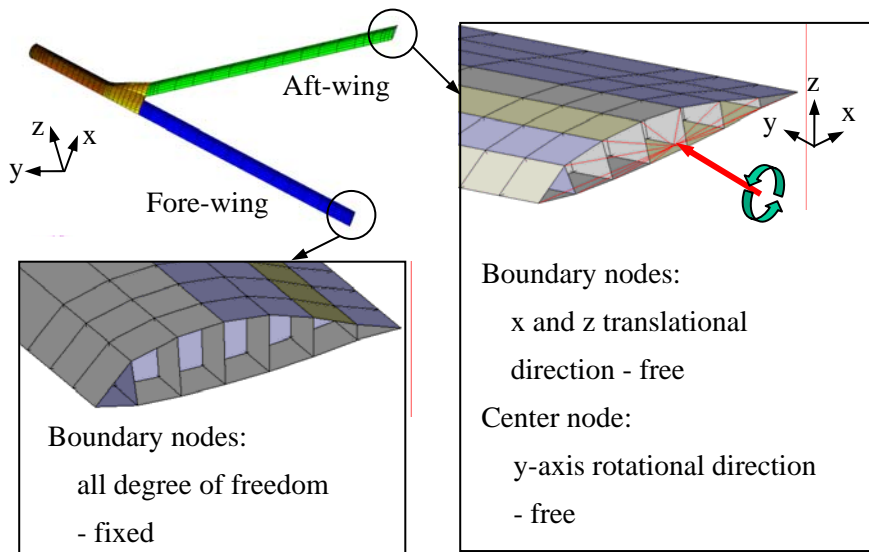
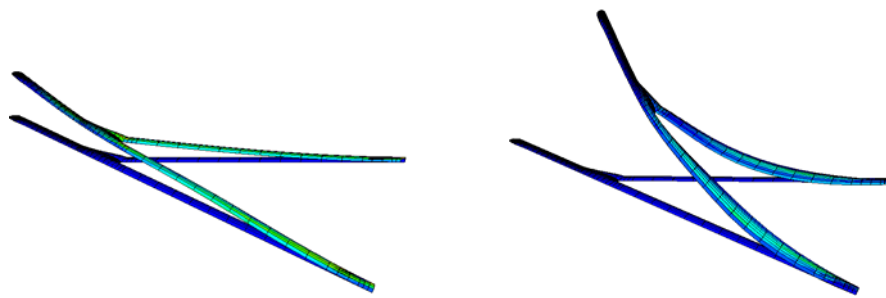


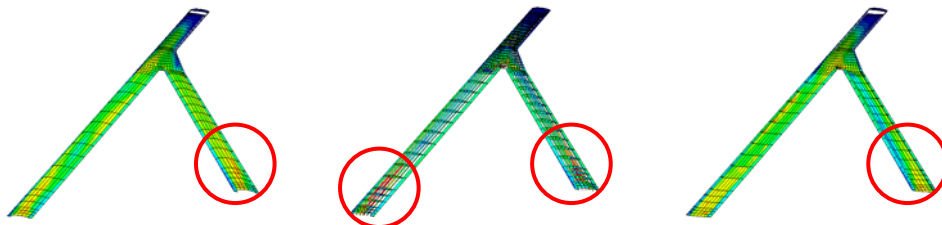
Fig. 6 Boundary conditions of the joined-wing



(a) Linear analysis

(b) Nonlinear analysis

Fig. 7 Deformation of the joined-wing under the gust loading condition

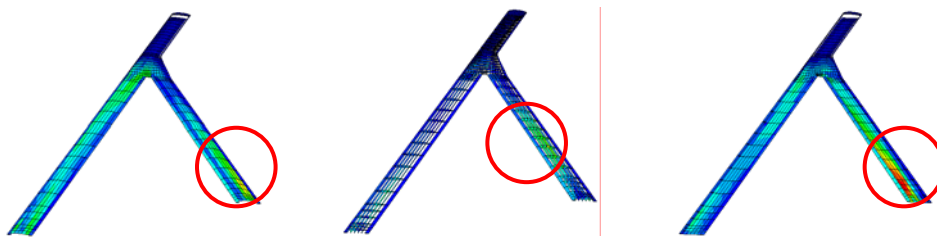


(a) Top skin

(b) Rib and spar

(c) Bottom skin

Fig. 8 Stress contours from linear analysis of a joined-wing



(a) Top skin

(b) Rib and spar

(c) Bottom skin

Fig. 9 Stress contours from nonlinear analysis of a joined-wing

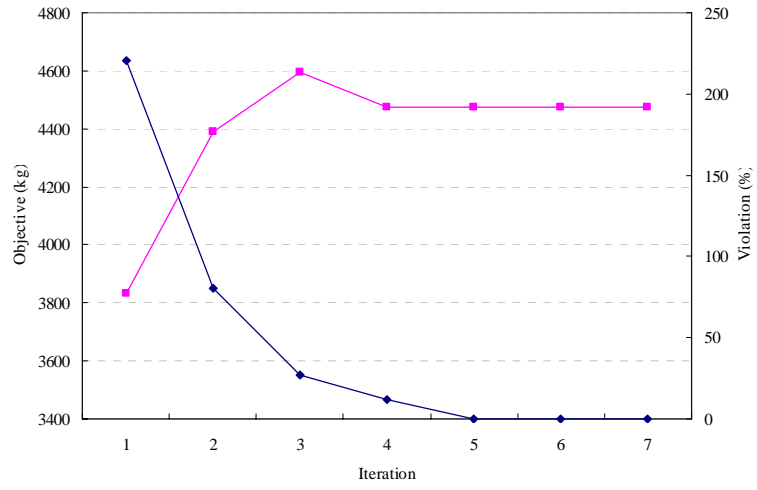


Fig. 10 History of linear response optimization

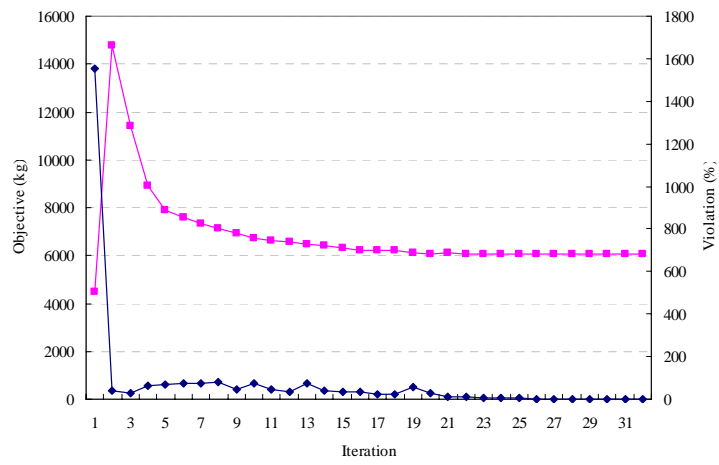


Fig. 11 History of nonlinear response optimization

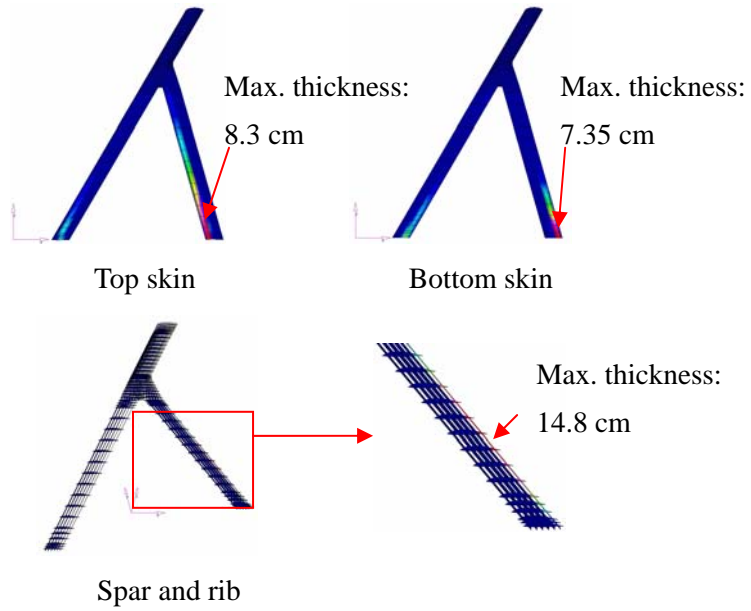


Fig. 12 Thickness contour of linear response optimization result

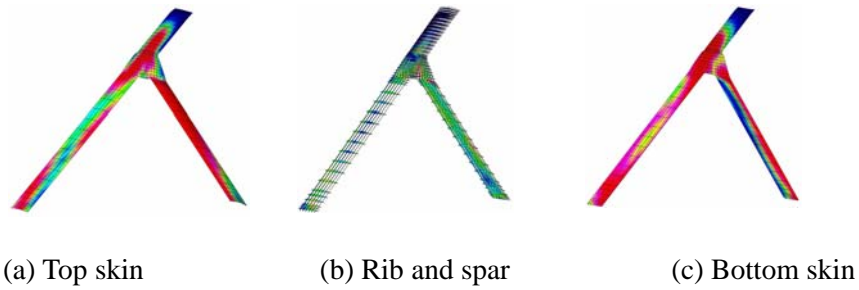


Fig. 13 Stress contours from linear analysis of the linear optimization result

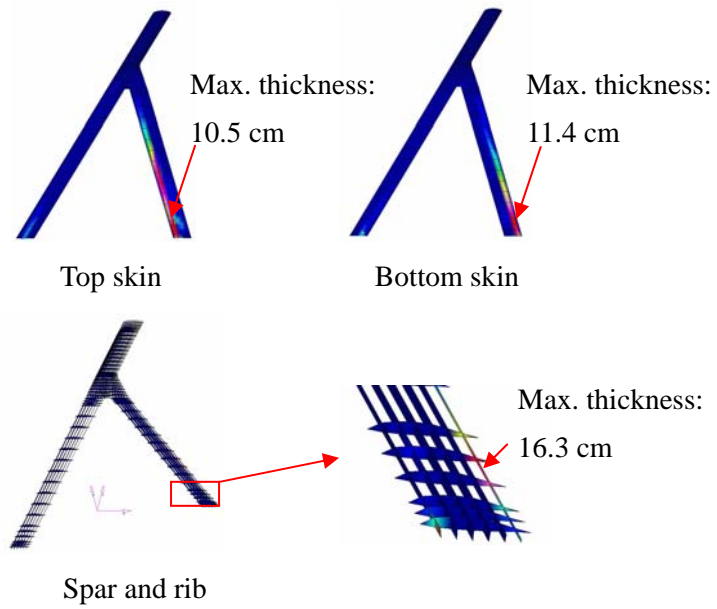


Fig. 14 Thickness contour of nonlinear response optimization result

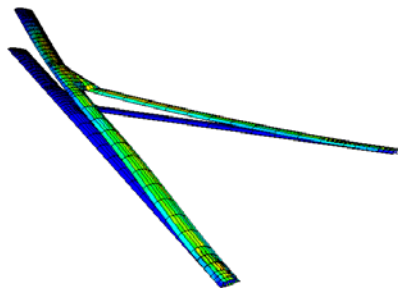


Fig. 15 Deformation of the optimum design

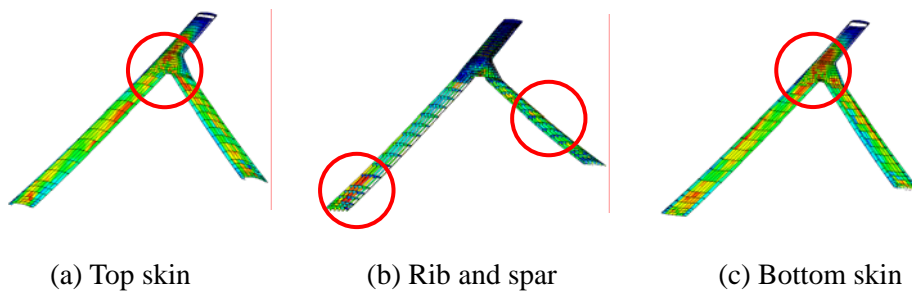


Fig. 16 Stress contours from nonlinear analysis of the optimum design

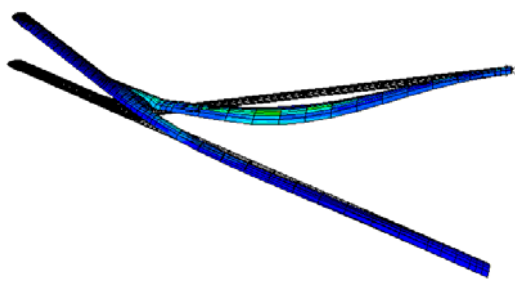


Fig. 17 Critical buckling mode for the cruise speed gust loading condition

Table 1 Loading conditions for optimization

Load no.	Load type	Mission leg
1	2.5g PullUp	Ingress
2	2.5g PullUp	Ingress
3	2.5g PullUp	Loiter
4	2.5g PullUp	Loiter
5	2.5g PullUp	Egress
6	2.5g PullUp	Egress
7	2.5g PullUp	Egress
8	Gust (Maneuver)	Descent
9	Gust (Cruise)	Descent
10	Taxi (1.75g impact)	Take-Off
11	Impact (3.0g landing)	Landing

Table 2 Wing tip displacements of the linear and nonlinear analyses

Number of loading condition	Wing tip displacement from linear analysis	Wing tip displacement from geometric nonlinear analysis
1	1.51 m	1.77 m
2	1.44 m	1.76 m
3	0.78 m	1.09 m
4	0.66 m	1.19 m
5	1.83 m	2.40 m
6	1.07 m	1.99 m
7	1.05 m	2.88 m
8 (gust: maneuver)	3.70 m	21.99 m
9 (gust: cruise)	4.62 m	23.03 m
10	-3.31 m	Did not converge
11	-0.54 m	-5.62 m

Table 3 Results of linear response optimization

Iteration no.	Optimization value (kg)	Constraint violation (%)
0	3832.0	220.8
1	4390.7	80.7
2	4593.6	27.3
3	4472.5	11.6
4	4475.2	0.0
5	4475.1	0.0
6	4475.0	0.0

Table 4 Results of nonlinear response optimization

Iteration no.	Optimization value (kg)	Constraint violation (%)
0	4475.0	1551.6
1	14752.3	42.3
2	11428.5	28.2
3	8907.3	62.7
4	7921.1	66.4
...
28	6073.9	0.5
29	6074.5	0.5
30	6066.1	0.0
31	6066.0	0.0

References

1. J. Wolkovich, 1986, "The Joined-Wing: An Overview," *Journal of Aircraft*, Vol. 23, No. 3, pp. 161-178.
2. H. Miura, A. T. Shyu, and J. Wolkovich, 1988, "Parametric Weight Evaluation of Joined Wings by Structural Optimization," *Journal of Aircraft*, Vol. 25, No. 12, pp. 1142-1149.
3. J. W. Gallman and I. M. Kroo, 1996, "Structural Optimization of Joined-Wing Synthesis," *Journal of Aircraft*, Vol. 33, No. 1, pp. 214-223.
4. M. Blair, R. A. Canfield and R. W. Roberts, 2005, "Joined-Wing Aeroelastic Design with Geometric Nonlinearity," *Journal of Aircraft*, Vol. 42, No. 4, pp. 832-848.
5. M. Blair and R. A. Canfield, 2002, "A Joined-Wing Structural Weight Modeling Study," 45th AIAA/ASME/ASCE/AHS/ASC Structures, Structural Dynamics and Materials Conference, Denver, CO, USA.
6. R. W. Roberts, R. A. Canfield and M. Blair, 2003, "Sensor-Craft Structural Optimization and Analytical Certification," 44th AIAA/ASME/ASCE/AHS/ASC Structures, Structural Dynamics and Materials Conference, Norfolk, VA, USA.
7. C. C. Rasmussen, R. A. Canfield and M. Blair, 2004, "Joined-Wing Sensor-Craft Configuration Design," 45th AIAA/ASME/AHS/ASC Structures, Structural Dynamics and Materials Conference, Palm Springs, CA, USA.
8. C. C. Rasmussen, R. A. Canfield and M. Blair, 2004, "Optimization Process for Configuration of Flexible Joined-Wing," 10th AIAA/ISSMO Multidisciplinary Analysis and Optimization Conference, Albany, NY, USA.
9. H. A. Lee, Y. I. Kim, G. J. Park, R. M. Kolonay, M. Blair, and R. A. Canfield, 2006, "Structural Optimization of a Joined-Wing Using Equivalent Static Loads," 11th AIAA/ISSMO Multidisciplinary Analysis and Optimization Conference, AIAA, Portsmouth, Virginia. (accepted by the *Journal of Aircraft*).
10. J. Katz, A. Plotkin, 1991, *Low-Speed Aerodynamics*, McGraw-Hill, NY.
11. R. D. Cook, D. S. Malkus, M. E. Plesha, and R. J. Witt, 2001, *Concepts and Applications of Finite Element Analysis, fourth edition*, John Wiley and Sons. Inc., NY.

12. J. N. Reddy, 2004, *An Introduction to Nonlinear Finite Element Analysis*, Oxford University Press., NY.
13. K. J. Bathe, 1996, *Finite Element Procedures*, Prentice-Hall, Inc., New Jersey.
14. F. M. Hoblit, 1988, *Gust Loads on Aircraft: Concepts and Applications*, American Institute of Aeronautics and Astronautics, Inc., Washington, DC, Chaps. 2, 3.
15. Y. S. Ryu, M. Haririan, C. C. Wu, and J. S. Arora, 1985, "Structural Design Sensitivity Analysis of Nonlinear Response," *Computers and Structures*, Vol. 21, No. 1/2, pp. 245-255.
16. C. C. Wu and J. S. Arora, 1987, "Design Sensitivity Analysis and Optimization of Nonlinear Structural Response using Incremental Procedure," *AIAA Journal*, Vol. 25, No. 8, pp. 1118-1125.
17. A. Suleman and R. Sedaghati, 2005, "Benchmark Case Studies in Optimization of Geometric Nonlinear Structures," *Structural and Multidisciplinary Optimization*, Vol. 30, pp. 273-296.
18. R. T. Haftka and Z. Gürdal, 1992, *Elements of Structural Optimization*, Kluwer Academic Publishers, Netherlands.
19. J. S. Arora, 2001, *Introduction to Optimum Design, International edition*, McGraw-Hill Book Co., Singapore.
20. G. J. Park, 2007, *Analytical Methods in Design Practice*, Springer-Verlag, Germany.
21. MSC. NASTRAN 2004 Reference Manual, 2004, MSC. Software Corporation, Santa Ana, CA.
22. M. K. Shin, K. J. Park. and G. J. Park, 2007, "Optimization of Structures with Nonlinear Behavior using Equivalent Loads," *Computer Methods in Applied Mechanics and Engineering*, Vol. 196, pp. 1154-1167.
23. Y. I. Kim, H. A. Lee and G. J. Park, 2006, "Case Studies of Nonlinear Response Structural Optimization using Equivalent Loads," *The Fourth China-Japan-Korea Joint Symposium on Optimization of Structural and Mechanical Systems, CJKOSM4*, Kunming, China.
24. K. J. Park and G. J. Park, 2004, "Structural Optimization of Truss with Nonlinear Response using Equivalent Linear Loads," *Transactions of the Korean Society of Mechanical Engineers (A)*, Vol. 28, No. 4, pp. 467-474. (in Korean)

25. ABAQUS/Standard Version 6.5, User's Manual, 2004, Hibbitt, Karlsson and Sorensen, Inc. Pawtucket, RI, USA.
26. GENESIS User's Manual, Version 7.0, 2001, Vanderplaats Research and Development, Inc., Colorado Springs, CO.
27. M. Waite, S. Prata and D. Martin, 1984, *C Primer Plus*, Sams & Co. Inc., USA.
28. Hewlett-Packard Development Company, L. P., URL: <http://www.testdrive.hp.com/current.shtml> [cited 20 March 2007]